Research article

# Comprehensive analyses of m1A regulator-mediated modification patterns determining prognosis in lower-grade glioma (running title: m1A in LGG)

Kunjian Lei [a,b,c,1], Yilei Sheng [b,c,d,1], Min Luo [a,e], Junzhe Liu [a,e], Chuandong Gong [a,e], Shigang Lv [a], Wei Tu [a], Minhua Ye [a], Miaojing Wu [a], Bing xiao [a], Hua Fang [a], Haitao Luo [a], Xinjun Liu [f], Xiaoyan Long [g], Xingen Zhu [a,b,c], Kai Huang [a,b,c], Jingying Li [h,*]

[a] Department of Neurosurgery, The Second Affiliated Hospital of Nanchang University, Nanchang, Jiangxi, 330006, China
[b] Jiangxi Provincial Key Laboratory of Nervous System Tumors and Cerebrovascular Diseases, Nanchang University, Nanchang, Jiangxi, China
[c] JXHC Key Laboratory of Neurological Medicine, Nanchang University, Nanchang, Jiangxi, China
[d] Nanchang University, Nanchang, Jiangxi, 330006, China
[e] Institute of Neuroscience, Nanchang University, Nanchang, Jiangxi, 330006, China
[f] People's Hospital of Yingtan City, Jiangxi Province, Yingtan, Jiangxi, 335099, China
[g] East China Institute of Digital Medical Engineering, Shangrao, Jiangxi, 334000, China
[h] Department of Comprehensive Intensive Care Unit, The Second Affiliated Hospital of Nanchang University, Nanchang, 330006, Jiangxi, China

## ARTICLE INFO

## ABSTRACT

N1-methyladenosine (m1A) modification is a crucial post-transcriptional regulatory mechanism of messenger RNA (mRNA) in living organisms. Few studies have focused on analysis of m1A regulators in lower-grade gliomas (LGG). We employed the Nonnegative Matrix Factorization (NMF) technique on The Cancer Genome Atlas (TCGA) dataset to categorize LGG patients into 2 groups. These groups exhibited substantial disparities in terms of both overall survival (OS) and levels of infiltrating immune cells. We collected the significantly differentially expressed immune-related genes between the 2 clusters, and performed LASSO regression analysis to obtain m1AScores, and established an m1A-related immune-related gene signature (m1A-RIGS). Next, we categorized all patients with LGG into high- and low-risk subgroups, predictive significance of m1AScore was confirmed by conducting univariate/multivariate Cox regression analyses. Additionally, we confirmed variations in immune-related cells and ssGSEA and among the high-/low-risk subcategories in the TCGA dataset. Finally, our study characterized the effects of MSR1 and BIRC5 on LGG cells utilizing Edu assay and flow cytometry to explore the effects of modulation of these genes on glioma. The results of this study suggested that m1A-RIGS may be an excellent prognostic indicator for patients with LGG, and could also promote development of novel immune-based treatment strategies for LGG. Additionally, BIRC5 and MSR1 may be potential therapeutic targets for LGG.

\* Corresponding author.
   *E-mail address:* jingyingli@ncu.edu.cn (J. Li).
[1] These authors contribute equally to this work.

## 1. Introduction

Gliomas, characterized by high mortality and recurrence rate, are the most common primary malignant brain tumors in worldwide, [1]. Lowergrade gliomas (LGG), which include WHO grade III and II, are primarily diagnosed in adults, and can progress to aggressive glioblastomas (WHO grade IV, GBM) [2,3]. The blood–brain barrier has limited the efficacy of conventional drug therapy, which has hindered the progress of neurological tumors treatment [4]. In addition, the efficacy of nonspecific therapies such as radiation and chemotherapy are limited [5]. Hence, discovering new therapeutic targets is imperative and explore their specific roles in the onset and development of gliomas.

More than 100 chemical modifications of RNAs have been discovered, such as N6-methyladenosine (m6A), N1-methyladenosine (m1A), 5-methylcytosine (m5C), and others [6]. N1-methyladenosine modifications are similar to m6A modifications, which are crucial post-transcriptional regulators of messenger RNA (mRNA) in living organisms, and these modifications can be categorized into methyltransferases ("writers"), and demethylases ("erasers"), and binding proteins ("readers") according to their biological functions [7–9]. Studies have shown that m1A modifications repress translation through interference with base pairing [8]. In contrast, other studies have suggested that m1A modifications accelerated translation through TRMT61B, a mitochondria-localized m1A methyltransferase [8,10]. Furthermore, m1A modifications can promote and regulate cancers [11]. The identified key modulators of m6A have been used to predict tumor prognosis, deepening the understanding of tumor biology and discovering more effective treatment strategies for tumor patients [12,13]. However, the modulators of m1A have not been well identified and utilized.

Recent research has focused on the tumor microenvironment (TME), which consists of extracellular components, stromal cells, and cancer cells [14,15]. Tumor-associated macrophages, myeloid derived suppressor cells, and regulatory T cells are among the various types of cells involved in the development of cancer. Consequently, these immunosuppressive cells limit effector T cell recruitment, inhibit NK (natural killer) activity, and inhibit antigen-presenting cells (APCs) from monitoring tumors effectively, reducing anti-tumor immune response [16]. The TME can be reprogrammed to initiate, grow, invade, metastasize, and respond to therapies, according to a study released recently [14]. Moreover, TME is confirmed as a key role in carcinogenesis [17], and modulation of the TME has shown promise as a strategy to treat cancer [15]. Moreover, researches have indicated that immune cells appear to play a role in tumor immune evasion, which may provide a new target for immunotherapy [18,19].

Studies have indicated that m6A modifications are important in the TME and immune therapy, which indicates that adjustment of m6A modification may have potential as a strategy to suppress tumor growth [20]. A study showed that m6A modifications mediated the CD8^{+} T cell antitumor response through the m6A-binding protein YTHDF1, which promoted translation of lysosomal cathepsins in DCs [21]. Moreover, YTHDF1, in combination with EIF3C, can inhibit ovarian cancer [22]. Several studies have shown that CD34/CD276 in the TME can dysregulate m6A modifications, resulting in immune escape [23]. However, the effects of m1A modifications on the TME have not been characterized. Hence, the objective of this research is to examine the impacts of disparities in m1A modification on the TME, identify m1A-related regulators in patients with glioma, investigate the influence of various pivotal controllers on the prognosis of glioma patients and the formation and progression of glioma cells, and ultimately offer potential targets for immunotherapy against cancer.

## 2. Methods

### 2.1. Data acquisition and preprocessing of publicly available datasets

We conducted a study where we explored publicly accessible datasets in databases such as The Cancer Genome Atlas (TCGA), Chinese Glioma Genome Atlas (CGGA, http://www.cgga.org.cn/), Gene Expression Omnibus (GEO, https://www.ncbi.nlm.nih.gov/geo/), and Genotype-Tissue Expression database (GTEx, https://gtexportal.org/home/datasets). Excluded from the TCGA cohort were LGG patients who had missing OS data or OS time less than 30 days. Information regarding mutation status, DNA methylation, and CNV of the TCGA cohort patients was acquired from the UCSC Xena website (https://xenabrowser.net/datapages/). In total, 2497 immune-related genes (IRGs) were obtained from the MSigDB (https://www.gsea-msigdb.org/gsea/msigdb/index.jsp) [24]. Table 1

**Table 1**
The basic clinical information for primary LGG patients in the TCGA, CGGA, and GEO datasets.

| Variable | | TCGA set (n=462) | | CGGA set (n=590) | | GEO set (n=234) | |
|---|---|---|---|---|---|---|---|
| Age | >=mid | 237 | 51.30% | 307 | 52.03% | 122 | 52.14% |
| | <mid | 225 | 48.70% | 283 | 47.97% | 112 | 47.86% |
| Gender | Male | 255 | 55.19% | 339 | 57.46% | 146 | 62.39% |
| | Female | 207 | 44.81% | 251 | 42.54% | 88 | 37.61% |
| Grade | WHO II | 222 | 48.05% | 270 | 45.76% | 89 | 38.03% |
| | WHO III | 240 | 51.95% | 320 | 54.24% | 145 | 61.97% |
| IDH1 | Wildtype | 83 | 17.97% | 415 | 70.34% | N/A | N/A |
| | Mutant | 379 | 82.03% | 136 | 23.05% | N/A | N/A |
| | N/A | N/A | N/A | 39 | 6.61% | N/A | N/A |
| 1p/19q | Codel | 307 | 66.45% | 452 | 76.61% | N/A | N/A |
| | Non-codel | 155 | 33.55% | 127 | 21.53% | N/A | N/A |
| | N/A | N/A | N/A | 11 | 1.86% | N/A | N/A |

presents the precise information regarding the LGG samples included in our study.A publicly accessible algorithm was utilized to convert the fragments per kilobase of transcript per million (FPKM) values to transcripts per million kilobase (TPM) values in the TCGA cohort [25,26]. The batch effect between five cohorts was eliminated using the R package 'SVA', and the algorithm for removing batch effects is mainly based on the ComBat method of Bayesian principle. By establishing a batch effect model and correcting the data, batch effects are eliminated [27].

### 2.2. Nonnegative Matrix Factorization for ten m1A regulators

To identify the crucial genes involved in m1A modification patterns in all LGG patients within the TCGA dataset, NMF clustering was conducted utilizing the 10 m1A regulators that were identified for subsequent analysis. The R package 'NMF' was performed to generate the connectivity matrix and components of the two clusters [28].

### 2.3. Generation of m1A gene signatures and construction and verification of m1AScore

We used 'limma' R package to confirm the m1A-related differentially expressed immune-related genes (DEIGs) among the five cohorts. LASSO regression (iterations = 1000) was applied to detect DEIGs with robust prognostic value, and finally 8 m1A-RIGs has been identified. We constructed m1AScore to assess the m1A modification patterns of each patient with LGG. The m1AScore was calculated for each patient using the following equation:

$$m1A\ Score = \sum_{i=1}^{n} Coef_i * x_i$$

$Coef_i$: the coefficient of each DEIG index, $x_i$: $\log_2$(TPM+1) value for each identified DEIG among all cohorts.

To confirm the prognostic significance of the m1AScore, we evaluated its value for each glioma patient in the TCGA (training) dataset as well as the CGGA and GEO (validation) datasets. We categorized patients in each dataset into low-risk or high-risk subgroups based on the m1AScore's median. To evaluate the differences in overall survival between the subgroups categorized as low-/high-risk, the log-rank test was employed. Both univariate and multivariate Cox regression analyses were used to assess the independent predictive value of m1AScore.

### 2.4. Gene-set enrichment analysis (GESA)

The classical hallmark gene sets from MSigDB were used to identify potential differential pathways between m1A modifications. Next, using GSEA analysis to explore distinct hallmark pathways in the two clusters. Based on 8 identified m1A-related DEIGs, we used R's clusterProfiler package to analyze gene-ontology (GO) and Kyoto Encyclopedia of Genes and Genomes (KEGG) [29].

### 2.5. Single-sample gene-set enrichment analysis (ssGSEA)

We downloaded gene sets, including 29 representative "immune signatures", from previous studies [30,31]. To quantify the infiltration level of most immune cell type in all LGG patients, a ssGSEA algorithm was performed to calculate the values by means of R package 'GSVA' [32]. The ssGSEA technique assesses the proportional enrichment of each gene set in the sample by comparing the gene expression data of each sample with a designated gene set (specifically, the immune cell gene set). The analysis of immune cell infiltration involved the use of ssGSEA to evaluate the proportionate presence of various immune cell categories in every sample.

### 2.6. Establishment and validation of the nomogram model

Performing the R package 'rsm' to complete establishment and verification of our nomogram. The nomogram included m1AScore, age of the patient, 1p/19q codeletion status, and WHO grade, which were identified as important factors in the multivariate analysis. Calibration plots were generated by the 'rms' R package.

### 2.7. Real-time quantitative PCR and Western Blotting

Western Blot (WB) and real-time qPCR were used as previously described [33]. In short, RIPA buffer (Solarbio, Beijing, China) was used to prepare protein from cells. Protein samples were loaded on 10%–12% SDS-PAGE gels separated, and subsequently transferred to PVDF membranes provided by Millipore. Afterwards, the membranes will be subjected to incubation at a temperature of 4 °C with particular primary antibodies, which consist of GAPDH (1:20,000, Proteintech), MSR1 (1:1,000, CST), and BIRC5 (1:500, Proteintech). Finally, the membranes were visualized utilizing the imaging system (5200 Multi Chemiluminescent, Tanon).

The SimplyP Total RNA Extraction Kit (Bio-Flux, China) was utilized to extract the total RNA from cells. Afterwards, the RNA was converted into cDNA using the riboSCRIPT Reverse Transcription Kit (RIBOBIO, China).The primers utilized in real-time quantitative PCR were as follows: GADPH: F primer, 5′-CTCACCGGATGCACCAATGTT-3′, R primer: 5′-CGCGTTGCTCACAATGTTCAT-3′; MSR1: F primer, 5′-GCAGTGGGATCACTTTCACAA-3′, R primer, 5′-AGCTGTCATTGAGCGAGCATC-3′; and BIRC5: F primer, 5′-AGGAC-CACCGCATCTCTACAT-3′, R primer: 5′-AAGTCTGGCTCGTTCTCAGTG-3′.
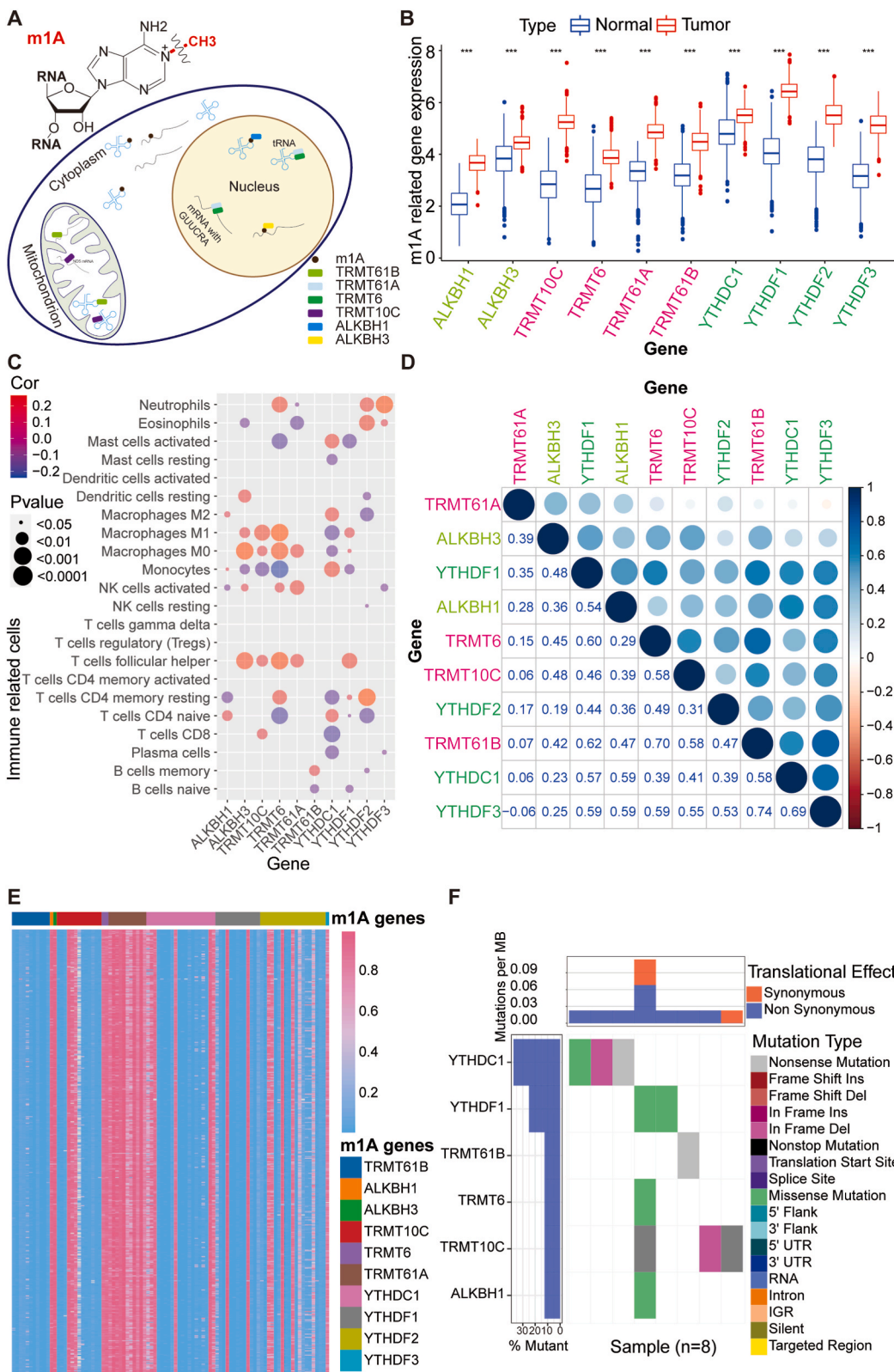
(caption on next page)

**Fig. 1.** The landscape of 10 m1A regulators in LGG based on the TCGA cohort. (A) Methylation and demethylation of m1A in tRNA and mRNA in cells. (B) Differential expression of m1A regulators between normal brain tissue and LGG following $\log_2(TPM + 1)$ transformation. The expression of these genes in tumor tissues was higher thanthat the expression in normal tissues. (C) Correlation between the 10 m1A regulators and immune related cells in LGG. Circles are not shown when $p > 0.05$. (D) Correlation between the 10 m1A regulators. The sizes of the circles represent the absolute values of the correlations. (E) Heatmap showing the methylation levels of the promoters of the 10m1A regulators. (F) The m1A regulators generally had a low mutation frequency in LGG.

### 2.8. Cell culture

SW1783 and SW1088 cell lines were acquired from American Type Culture Collection (ATCC). The Culture Collection of the Chinese Academy of Sciences (Shanghai, China) provided a sample of normal human astrocytes (NHA) cells. DMEM with 10% fetal bovine serum (FBS; Gibco) was used for culturing all cells. all cells were cultured in a 37 °C constant temperature incubator containing 5% $CO_2$.

### 2.9. Generation of shRNA and transfection

Lentivirus shRNA plasmids were purchased from Sigma. Three shRNAs targeting human MSR1 were designed, including shMSR1-1: 562–582 (GAGAGAGATCCAGCATATT) corresponding to coding sequences (CDSs), shMSR1-2: 245–265 (GCTGCTCCGAATCGT-GAAAT) corresponding to CDSs, and shMSR1-3: 1173–1193 (GCCAGGAAATTCTGGACCAAA) corresponding to CDSs. Lipofectamine 3000 (Thermo Fisher) was utilized to transfect cells fbased on the manufacturer's instructions.

### 2.10. Flow cytometry

To perform the apoptosis assay, we utilized the Annexin V and PI Apoptosis Kit (US EVERBRIGHT, USA) as per the specified guidelines. Initially, SW1088 was treated with EDTA-free trypsin (beyotime, China) for digestion. The resulting cells were subsequently washed twice with pre-cooled PBS. Afterwards, the cells were resuspended in $1 \times$ binding buffer and Annexin V and PI working solution were added sequentially to each centrifuge tube. After 15 min of incubation at room temperature, remove from the dark, and complete the detection on the flow cytometer as soon as possible after adding 400 µl of PBS.

### 2.11. Statistical analyses

The survival outcomes of LGG patients with high and low m1AScore were compared using the Kaplan-Meier (KM) method and the two-sided log-rank test. The m1AScore's predictive ability was evaluated using a time-dependent receiver operating characteristic (ROC) model, and the areas under the curve (AUC) were calculated using the R package 'pROC'. The prognostic significance of the m1AScore was determined through univariate and multivariate Cox regression analyses in all cohorts. Statistical significance was determined using two-sided P values, with a significance level of $p < 0.05$. Statistical analyses were constructed by the SPSS Statistics software (version 25, https://www.ibm.com/products/software) and R program language (version 4.0.1, https://www.r-project.org/).

## 3. Results

### 3.1. The landscape of m1A regulators in lower-grade glioma

Ten m1A regulators, including two erasers (ALKBH3 and ALKBH1), four writers (TRMT10C, TRMT61A, TRMT6, and TRMT61B), and four readers (YTHDF1, YTHDF2, YTHDF3, and YTHDC1) and, have been shown to regulate multiple cancers [11]. The simplified process of methylation and demethylation of m1A in cells was displayed in Fig. 1A. To determine differences in expression of the 10 m1A regulators in normal brain and LGG tissues in the GTEx and TCGA databases, we performed a $\log_2(TPM+1)$ transformation and differential expression analysis, this is because the TPM value can be directly compared between different samples, while FPKM can only be compared after further correction, which makes TPM more advantageous in aspects such as differential expression analysis. All m1A regulators revealed significantly increased expression in the results ($p < 0.001$) in LGG (Fig. 1B–S1A). Subsequently, we examined the association between infiltration of immune cells and the expression of genes related to m1A.The findings (Fig. 1C–S1B) indicate a notable correlation between the presence of m1A regulators and the infiltration of monocyte-macrophages. (Fig. 1C–S1B). The 10 m1A regulators evaluated in this study were mostly positively correlated with each other, with Cor>0.3, which indicated that some of these genes may have been co-expressed (Fig. 1D). However, the correlation between TRMT61A and other genes was generally weak. As shown in Fig. 1E, ALKBH1, ALKBH3, TRMT6, and TRMT61A were all highly methylated ($\beta > 0.8$). However, the m1A regulators showed a lower mutation rate in LGG (Fig. 1F). Analysis of copy number variation of m1A regulators showed that TRMT10C, TRMT6, YTHDF2, and YTHDF1 were amplification regulators, while TRMT61A, ALKBH3, and YTHDC1 were mainly deletion regulators (Fig. S1C).

### 3.2. Construction of differential modification patterns of m1A regulators

In the TCGA cohort, to classify the different clusters of m1A regulators, we used NMF and distinguished Cluster 1 and Cluster 2 using the most coincident k value (k = 2) after analyzing the cophenetic correlation coefficients (Fig. 2A, B, S2A). We generated a heatmap displaying the mRNA expression level of all 10 m1A regulators in clusters 1 and 2 (Fig. S2B). To further detect the potential relationship between prognosis and the two m1A modification patterns in patients with LGG, survival analysis was used. The findings indicated that Cluster 1 was linked to a higher likelihood of poorer OS or progression-free survival (PFS) in individuals diagnosed with LGG in the TCGA group (Fig. 2C and D).To identify differential cellular pathways or processes between the two m1A modification patterns, enrichment score was analyzed using GSEA (Fig. 2E and F).Cluster 2 had a higher representation of
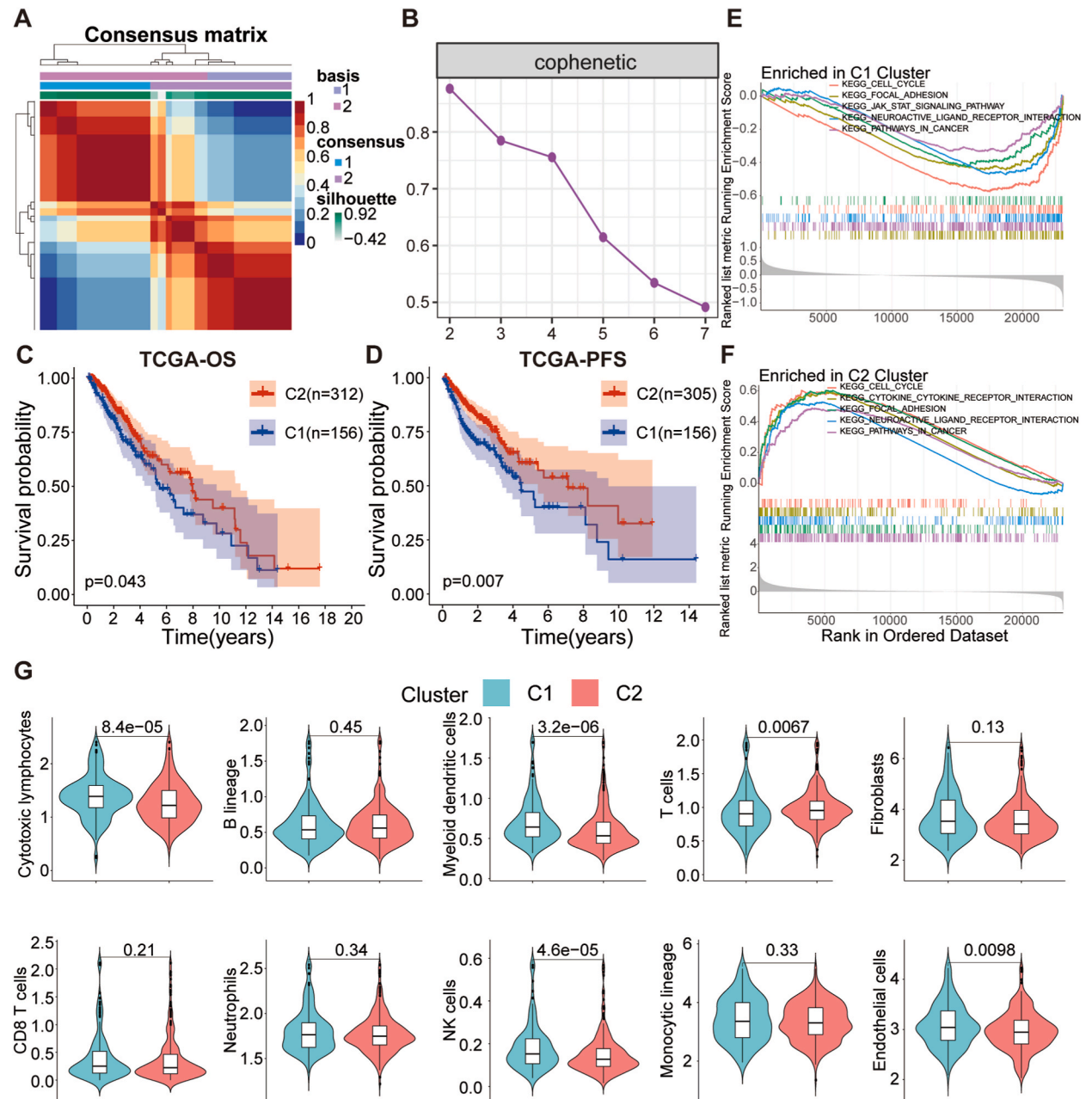


**Fig. 2.** NMF for m1A modification patterns, biological processes, and differences in immune cell infiltration. (A, B) Consensus matrix and cophenetic analysis for patients with LGG in the TCGA cohort, as determined using NMF. (C, D) Overall survival and PFS analysis between the two clusters in the TCGA cohort. Cluster 2 generally has longer OS or PFS than Cluster 1. (E, F) GSEA analysis for each modification pattern in the TCGA cohort. (G) Differential immune cell infiltration between the Cluster 1 and Cluster 2.
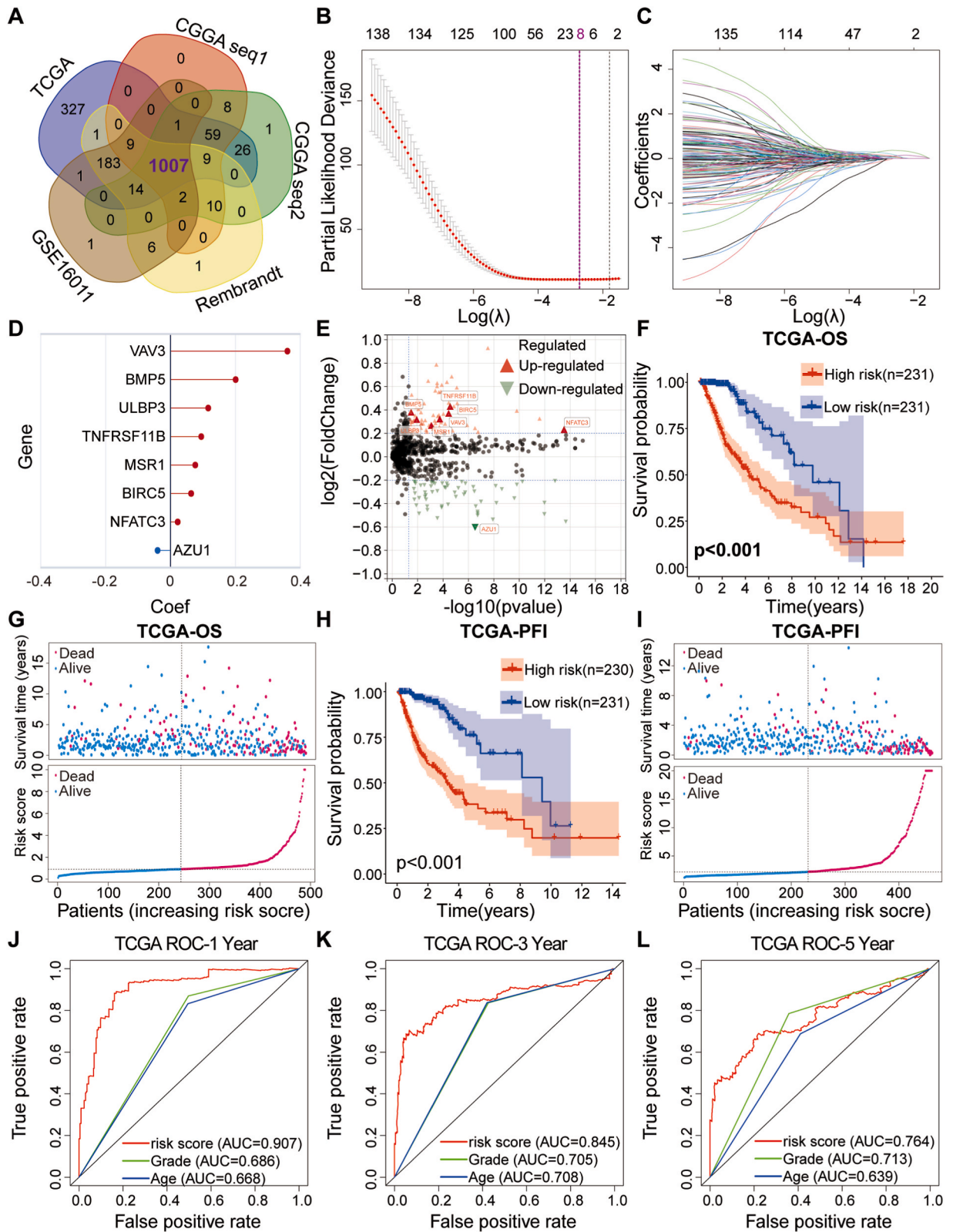
**Fig. 3.** Construction of m1A related immune-related genes Signatures (m1A-RIGS) using data from patients with LGG from TCGA. (A) Venn plot displaying the screened 1007 IRGs in all five cohorts. (B–D) LASSO regression was performed to determine the minimum criteria (A, B) and co-efficients. (E) The volcano map shows differential expression of each immune-related gene between the high- and low-risk subgroups. The 8 screened genes were all differentially expressed between the two subgroups (p < 0.0001). (F–I) K-M survival curves showed that the high-m1AScore group had worse OS or PFS than the low-m1AScore group in the training cohort. Survival status and distribution scatter plots of m1AScores of patients with LGG in the TCGA cohort. (J–L) ROC curves for m1A-RIGS to predict the 1-/3-/5-year survival outcome in the training cohort.

'JAK_STAT_SIGNALING_PATHWAY', 'CELL_CYCLE', and 'PATHWAYS_IN_CANCER' according to the results. The relative levels of immune cell infiltration between the two m1A modification patterns differed significantly in the TCGA cohort (p < 0.05). Furthermore, the patients with glioma in Cluster 2 had higher enrichment scores among most of the immune infiltration cells (p < 0.05), including
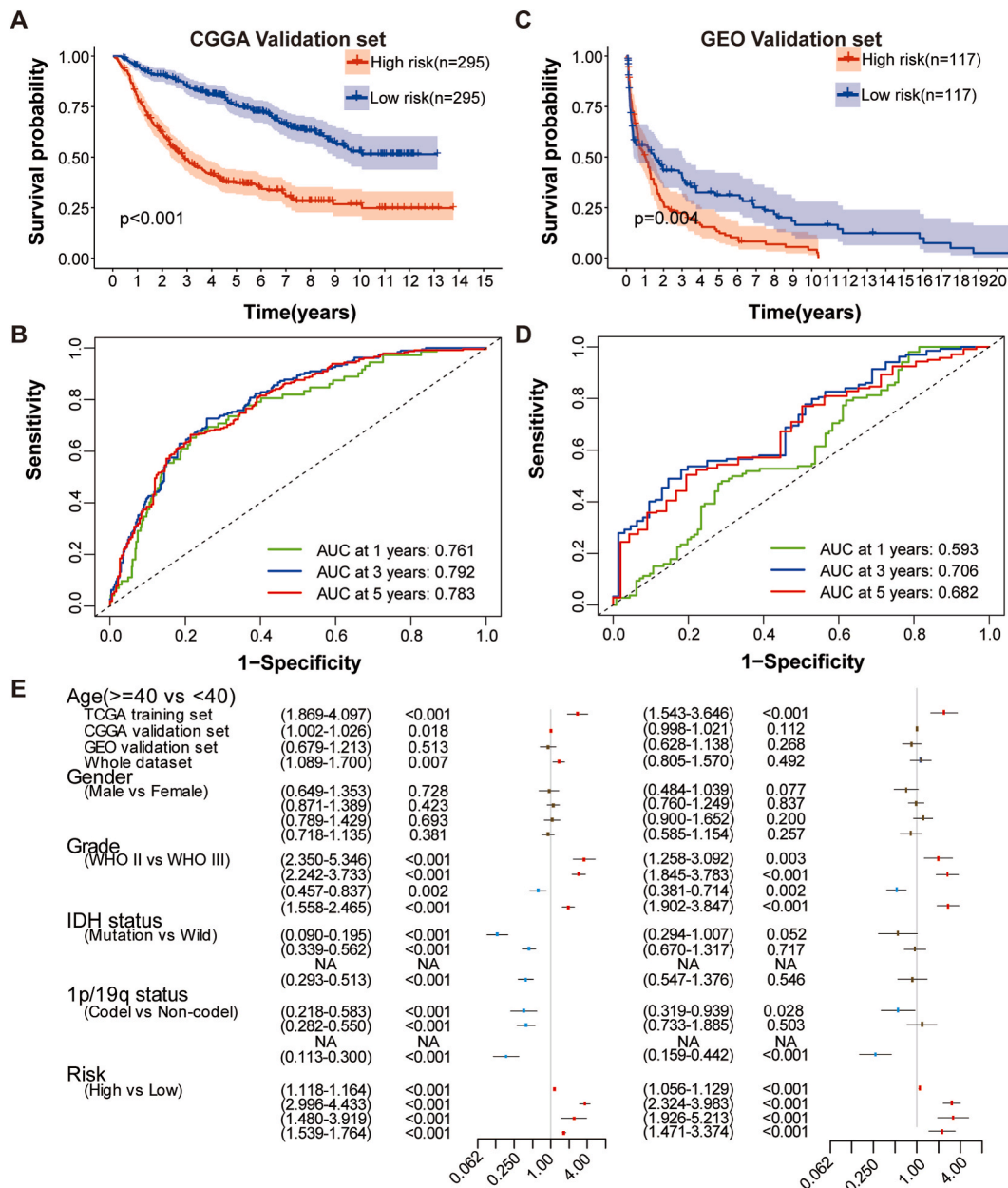


**Fig. 4.** Verification of m1A-RIGS in the CGGA and GEO datasets, and univariate and multivariate Cox analyses of clinical characteristics in all cohorts. (A–D) Survival analysis was performed using for all patients with LGG divided into high- and low-m1AScore subgroups using m1A-RIGS for the CGGA and GEO cohorts (A, C). ROC curves for the ability of m1A-RIGS for predicting 1-/3-/5-year survival outcome in the CGGA and GEO cohorts was performed (B, D). (E) Univariate and multivariate Cox analyses of multiple clinical and molecular features in all datasets.
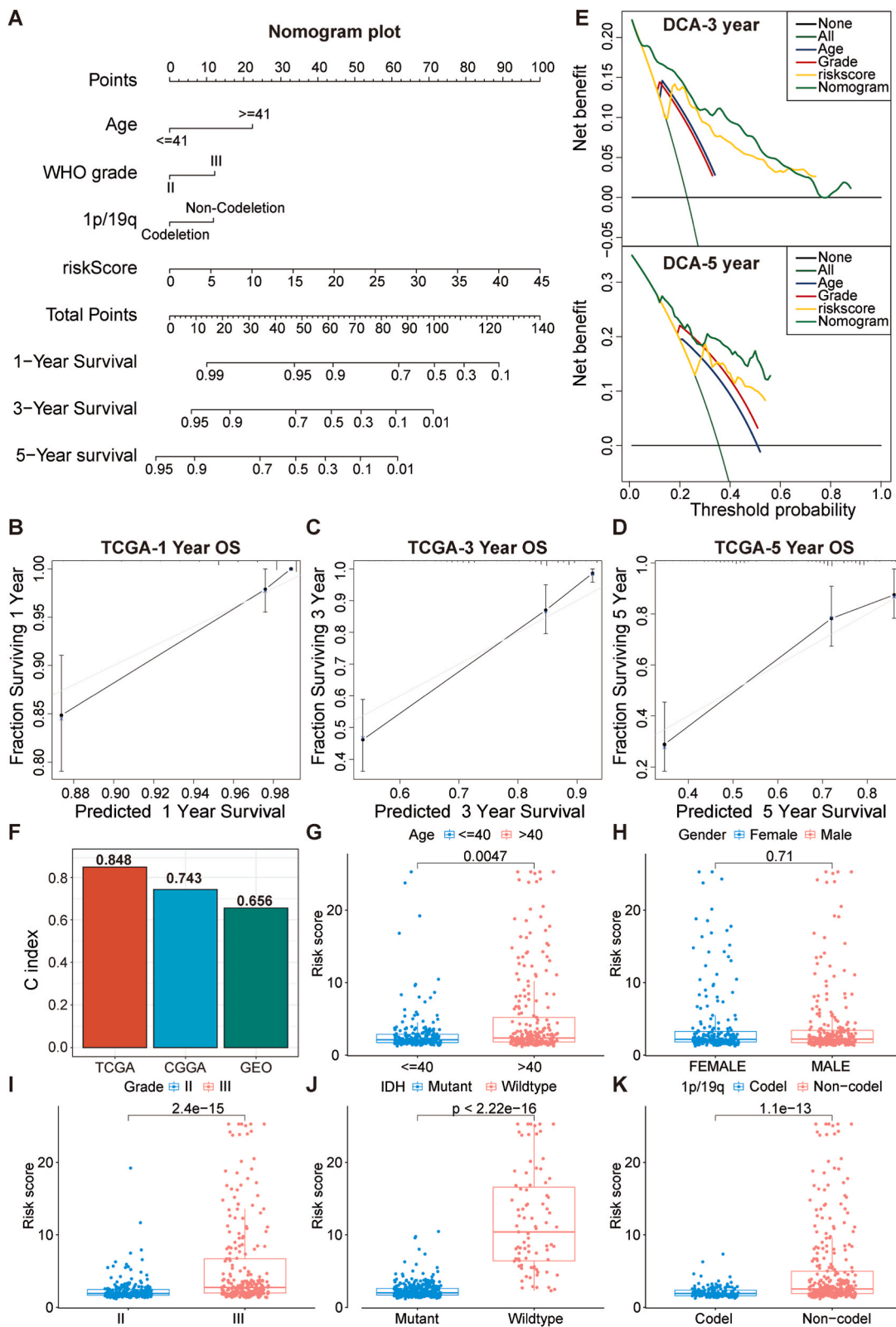
*(caption on next page)*

**Fig. 5.** Construction of a nomogram and analysis of differences in clinical information between the low- and high-m1AScore subgroups. (A) Nomogram model was built to predict the overall survival (OS) of LGG patients. (B–D) Calibration curves were used to predict the OS probability among LGG patients in the training dataset. (E) DCA was performed to determine the clinical benefits under each strategy. (F) The C-index of nomogram model in the TCGA dataset and the validation cohorts. (G) The box plot shows the difference of m1AScore among different clinical features. Except for gender, there were significant differences in the distributions of m1AScore and other clinical features in patients with LGG.

but not limited to, T cells, neutrophils, and CD8$^+$ cells (Fig. 2G).

### 3.3. Detection of differentially expressed genes (DEGs) among 2 m1A alteration patterns and development of an m1A-associated immune-related gene signature (m1A-IRGS)

In the combined analysis, 1007 shared m1A-RIGs were extracted from five databases using a Venn diagram (Fig. 3A). To further analyze the data, we selected the TCGA dataset as the training chort and performed a difference analysis to detect DEIRGs (p < 0.05, | LogFC|>0.25) between Cluster 1 and Cluster 2, and obtained 139 m1A-RDEIGs. To determine the most important OS-related m1A-RDEIG for construction of an m1A-related immune-related gene signature, and then we utilized LASSO-Cox regression analysis, which resulted in identification of 8 m1A-RIGs, including VAV3, BMP5, ULBP3, TNFRSF11B, MSR1, BIRC5, NFATC3, and AZU that correlated with patient prognosis (Fig. 3B–D). In addition, we built an equation to determine the relationship between m1AScore and OS outcomes, and screened for OS-related m1A-RDEIGs. This analysis resulted in assignment of 1 negative and 7 positive genes (Fig. 3D). A volcano plot was generated and shows the positions of these 8 genes among all of the immune-related genes that were evaluated, only AZU1 was down-regulated in tumor patients, while the other seven genes were up-regulated in tumor tissues (Fig. 3E).

In order to investigate the relationship between the m1AScore and the likelihood of survival in LGG patients, we utilized the median m1AScore as a threshold to categorize all patients into subgroups with low and high risks, using the TCGA cohort. The results suggested that patients with LGG in the low-risk group had better prognoses overall and PFS (Fig. 3F–I, p < 0.001). These results indicated that glioma patients in high-risk group had poorer survival after treatment and a higher degree of disease deterioration. The survival status and m1AScore distributions of each LGG patient are shown in Fig. 3G and I.ROC curves were conducted to examine the prognostic capability of m1A-RIGS and validate the predictive value of the data for OS based on the m1AScores obtained from the TCGA dataset (Fig. 3J-L).

### 3.4. Verification of m1A-RIGS

After building a prognostic model using the TCGA dataset, two external validation datasets: the CGGA cohort (CGGA seq1 and CGGA seq2) and the GEO cohort (GSE16011 and Rembrandt) had been merged. The m1AScore of each patient in the validation set was evaluated by determining their m1AScores to confirm the prognostic value of m1A-RIGS. The CGGA and GEO cohorts classified all LGG patients into high-risk or low-risk subgroups according to m1AScores. These independent validation datasets showed similar results obtained from the training dataset (Fig. 4A–D). Survival analysis and ROC curves revealed that patients with LGG in the high-risk subgroup generally had lower survival rates. Furthermore, the ROC curves demonstrated that m1A-RIGS offered a dependable approach for forecasting OS in both the CGGA and the GEO groups. Moreover, in order to identify consistent and influential prognostic factors, a comprehensive analysis was conducted using univariate and multivariate Cox regression analyses. This analysis encompassed various clinical and pathological characteristics such as sex, age, WHO grade, IDH mutation status, and the status of 1p/19q co-deletion. Based on the m1AScores, calculations were performed to determine P-values, hazard ratios (HR), and 95% confidence intervals. The results of the Multivariate Cox analysis indicated that survival in the TCGA dataset was linked to age, 1p/19q co-deletion status, WHO grade, and m1AScore. However, only m1AScore demonstrated a strong and dependable prognostic association in all cohorts (p < 0.001, HR = 2.228, 95% CI: 1.471–3.374).

### 3.5. Construction and validation of nomogram model

Age is an established risk factor for patients with glioma [34]. Therefore, to generate a reliable model to predict OS in patients with LGG, and to analyze the prognostic value of m1A-RIGS, a nomogram was generated using age, WHO grade, 1p/19q codeletion status, and m1AScore (Fig. 5A). The results showed that m1AScores was good predictors of survival, and significantly outperformed the other two factors. To validate the accuracy of the predictive data, calibration plots were used, which indicated that the nomogram was well-calibrated across all datasets (Fig. 5B–D). Furthermore, the clinical advantages of the various approaches were assessed using decision curve analysis (DCA) (Fig. 5E). The results displayed that the nomogram and m1A-Score have good reliability than others independent predictive variables according to 3- and 5-year DCA curves. These results were similar to those obtained from analyses of the TCGA dataset and the two validation cohorts (Figs. S3A and S3B). The C index, reflects the model prediction accuracy, indicated agreement among the three cohorts (Fig. 5F). These findings demonstrated that m1A-RIGS-based nomogram models were for the most robust models for predicting patient outcomes. In order to assess the impact of clinicopathological characteristics on m1AScores in individuals diagnosed with LGG, we investigated the correlations among different factors such as patient age, WHO grade, the m1AScore, status of 1p/19q co-deletion, and IDH mutation status. The results showed that individuals with LGG who had a grade III according to WHO, co-deletion status of 1p/19q, and IDH wildtype had higher m1AScores (Fig. 5G–K).

### 3.6. GSEA analysis and correlation of m1A-related phenotypes with immune cell infiltration

In order to examine the possible biological roles of m1A-RIGS, a differential analysis was conducted to identify DEGs (|log2 (Fold-Change) | > 1, p < 0.05) between the high-/low-risk groups of patients with LGG in the TCGA cohort. We used "clusterProfiler" R package to perform GO, GSEA,and KEGG analyses according to the screened DEGs. The identified DEGs were enriched in cancer-
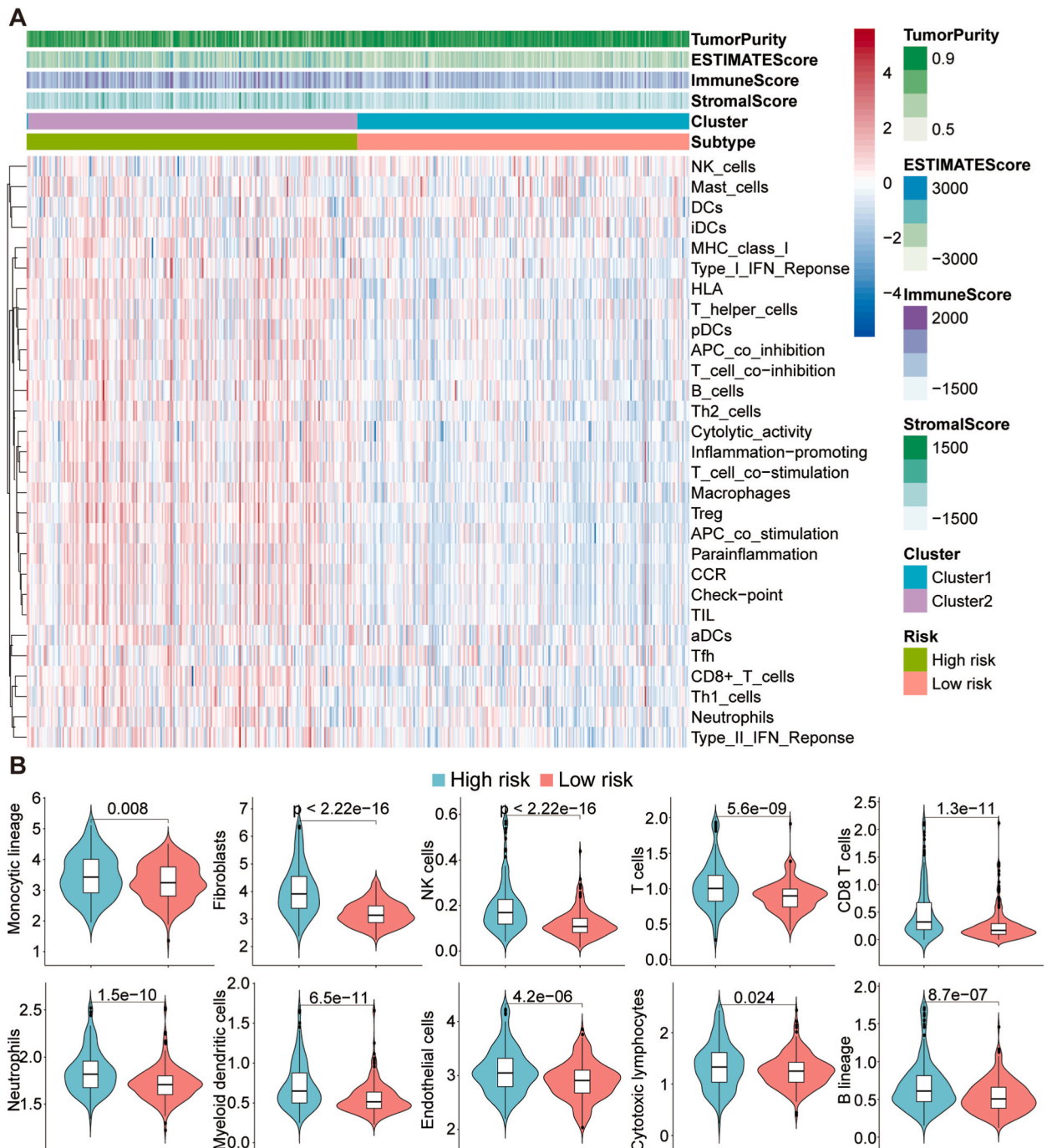


**Fig. 6.** The ssGSEA analysis of the high- and low-m1AScore subgroups determined using m1A-RIGS, differences in immune infiltrating cells, and benefits associated with radiotherapy and chemotherapy. (A) Patients with lower-grade gliomas (LGG) were divided into high- and low-m1AScore subgroups based on m1A-RIGS. Immune scores, stromal scorestumor purity, and ESTIMATE scores were determined using the ESTIMATE algorithm for each patient with LGG. (B) All selected immune cell showed differential infiltration between the high- and low-m1AScore subgroups (P < 0.05).
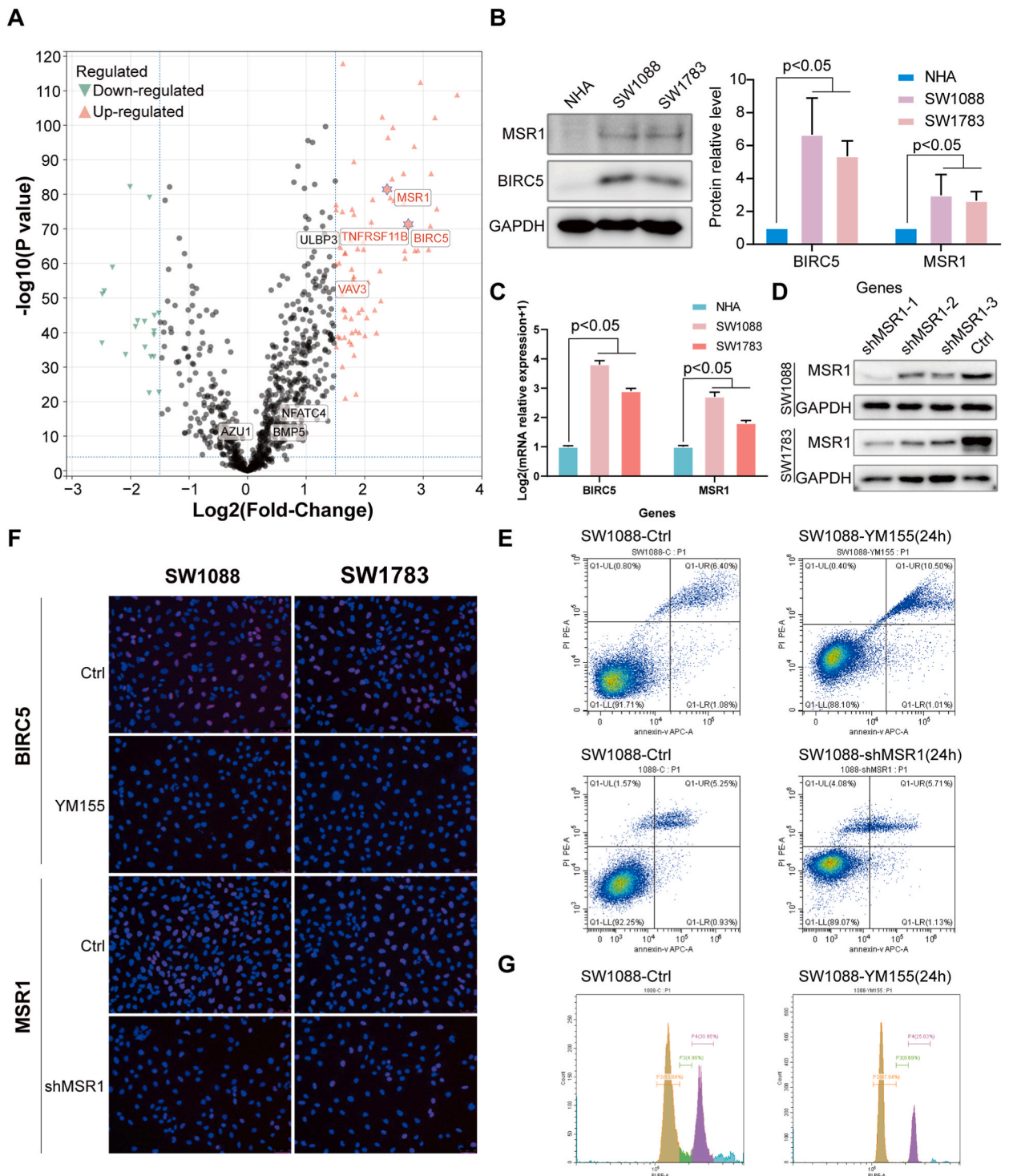
**Fig. 7.** Evaluation of the impact of MSR1 and BIRC5 on LGG cells. (A) The volcano map showed the differences in expression of each immune-related gene between LGG and GBM. The results showed that MSR1 and BIRC5 were both differentially expressed between LGG and GBM (p < 0.0001, |LogFC|>1.5). (B) Western blot analysis was performed to quantitate MSR1 and BIRC5 protein levels in NHA, SW1088, and SW1783 cells. *P < 0.05. (C) Quantitative RT-PCR analysis of MSR1 and BIRC5 in NHA, SW1088, and SW1783 cells. Expression was normalized against glyceraldehyde 3-phosphate dehydrogenase (GAPDH) mRNA expression. *P < 0.05. (D) Efficiency of MSR1 knockdown after transfection of cells with three shMSR1. (E) Flow cytometry was used to evaluate changes in apoptosisin SW1088 cells in response to YM155 treatment and shMSR1. (F) Edu assay showed that YM155 and shMSR1 treatment significantly reduced proliferation of SW1088 and SW1783 cells. (G) Flow cytometry was used to evaluate changes in cell cycle of SW1088 cells in response to YM155 treatment.

related biological function, including 'gastric cancer', 'breast cancer', 'MAPK signaling pathway', and 'response to transforming growth factor beta', and many immune-related pathways (Figs. 4A–4C). These results indicated that m1A-RIGS and immune cell infiltration were associated. To characterize this potential association, we used the ssGSEA algorithm. Significant disparities ($p <$ 0.001) were observed ($p < 0.001$) in tumor purity, ESTIMATE scores, immune scores, and stromal scores between the high-low-risk subgroups (Fig. 6A). In addition, all 29 representative "immune signatures" also showed considerable differences between the two subgroups ($p < 0.001$).

We selected several classic immune-related cells for analysis, and grouped the immune cell infiltration pattern of each patient with LGG according to high-/low-risk (Fig. 6B). The extent of infiltration of immune-related cells in the low-risk subgroup was significantly reduced ($p < 0.05$), suggesting potential variations in the immune microenvironment and immune regulation among the high-risk and low-risk subgroups. The enrichment of specific immune cells was also used to further characterize LGG. Regulation of immune cells may be prospective in preventing or managing tumors.

### 3.7. Effects of m1A-related immune-related genes on development of LGG

For the 8 genes screened, we performed survival analysis on LGG patients in the training dataset. The two subgroups showed significant variations in the expression of all 8 genes ($p < 0.05$) (Fig. S5). This further confirmed that the genes in our m1A-RIGS were good prognostic indicators for patients with LGG. Previous studies have indicated that LGG may develop into GBM, which has a higher degree of malignancy, and often involves abnormal activation, amplification, or down-regulation of some genes. To further explore whether 8 genes were significantly different expression between LGG and GBM patients, we used volcano plots to show the expression level differences of the 8 m1A-RIGS genes identified in our study among all immune-related genes between LGG and GBM patients (Fig. 7A). Patients with LGG and GBM exhibited notable variations in mRNA expression for MSR1 (CD204), BRIC5 (Survivin), TNFRSF11B, and VAV3, which were significantly distinct ($|LogFC|>1.5$, $p < 0.0001$). We hypothesized that overactivation or increased expression levels of MSR1 and BIRC5 could promote malignant behavior in LGG.Evidences have revealed that BIRC5 can promote cell proliferation and anti-apoptosis in gliomas [35]. MSR1 is a marker of M2 macrophages, and has been shown higher expression in patients with gbm compared to those with grade II gliomas, which indicated that MSR1 may exert cancer-promoting effects [36,37]. To verify the screened robust m1A-RDEIGs (MSR1 and BIRC5) in LGG and corresponding normal cell lines. We quantitated the protein and mRNA levels (Compare with the value of $2^{-\Delta\Delta Ct}$) of MSR1 and BIRC5 in normal human astrocytes (NHA), and in SW1088 and SW1783 lower-grade glioma cells (Fig. 7B and C). The findings indicated that LGG cells exhibited higher expression levels of MSR1 and BIRC5 compared to NHA cells. As BIRC5 may promote cell proliferation via inhibition of apoptosis, we used YM155, a specific inhibitor of BIRC5, to inhibit the expression of BIRC5. Meanwhile, to further study the effects of MSR1 in LGG cells, we designed shRNAs targeted to MSR1, and successfully verified knockdown of MSR1 (Fig. 7D). And we selected shMSR1-1 for further experiments. The results from flow cytometry analysis displayed a significant increase of apoptotic cells number following inhibition of BIRC5 ($p < 0.05$). This indicates that BIRC5 might contribute to cancer promotion by suppressing apoptosis in LGG cells (Fig. 7E). We also evaluated the effect of YM155 by Edu analysis, and inhibition of BIRC5 reduced the cell proliferation rate and S phase (Fig. 7F and G). Downregulation of MSR1 in SW1088 cells indicated that MSR1 inhibited apoptosis to a lesser extent than BIRC5 (Fig. 7E). However, knockdown of MSR1 significantly inhibited cell proliferation (Fig. 7F). In summary, up-regulation of MSR1 and BIRC5 was associated with cancer-promoting effects in LGG, and may be key control nodes in some signaling pathways. Therefore, BIRC5 and MSR1 may be potential therapeutic targets for LGG.

## 4. Discussion

Limited research has provided insights into the involvement of m1A alteration, a type of modification occurring after transcription, in the progression of tumors. The development of tumors and the advancement of tumors can be affected by this form of alteration. In our investigation, we extensively examined the pattern of m1A controllers in LGG and methodically depicted the infiltration of immune cells into the tumor microenvironment (TME), which was facilitated by the combined effects of several m1A controllers and alterations. In addition, we built m1AScore, a scoring system to evaluate the m1A modification pattern in each patient with LGG, to aid in determination of prognosis. The purpose was to develop a clinical tool for personalized and effective anti-tumor immunotherapy.

We examined the levels of mRNA expression, copy number variation, correlations, methylation levels, and mutation status of these m1A regulators in the study. Most of these regulators showed significant positive correlations in their expression levels. Interestingly, each of the 10 m1A regulators were overexpressed in LGG. Next, we placed the patients into two clusters using the NMF clustering method to identify different modification patterns with significant features associated with m1A regulators. We performed GSEA analysis and found that many dynamic processes, such as 'cell cycle,' 'cytokine receptor interaction,' and 'pathways in cancer,' were markedly enriched in Cluster 2. These results indicated that m1A regulators profoundly influenced the immune microenvironment and LGG development.

Previous studies have shown that modulation of m1A regulators could benefit cancer therapy. A study showed that m1A levels in HTRM6P/HTRM61P in bladder urothelial carcinoma tissue were associated with progression of bladder urothelial carcinoma [38]. Furthermore, m1A regulators have been shown to modulate the ErbB2 and mTOR pathways in gastrointestinal cancer [39]. Another study showed that ALKBH3 promoted carcinogenesis through interaction with angiogenin (ANG) and production of tRNA-derived small RNAs [40]. These studies showed that intracellular m1A regulators or m1A levels may be promising targets for novel anti-tumor drugs.

Recent studies have examined the relationship between m1A modifications and immune cell infiltration. Low m1AScore was

associated with CD8$^{+}$ T effector proliferation, high MSI, neoantigen burden, and PD-L1 expression, which was associated with inhibition of colon cancer [41]. In addition, m1A methylation mediated ovarian cancer progression through modulation of immune cell infiltration [42]. Moreover, the expression of TRM6/TRM61 mRNA was reduced in highly aggressive glioblastoma compared with that in WHO Grade II/III gliomas, which indicated that modulation of m1A modification may be a promising therapeutic strategy for glioma [43].

To further evaluate the prognostic power of m1AScore in LGG patients, we constructed an m1A-RIGS using differentially expressed m1A-related immune-related genes from the TCGA dataset. The validation of this analysis involved the utilization of m1A-RIGS to differentiate between high-/low-risk subgroups in the GEO and CGGA datasets. Furthermore, a nomogram was built incorporating four factors: the presence of 1p/19q co-deletion, patient age, WHO grade, and m1Ascore, in order to evaluate the predictive ability of m1A-RIGS.The results showed that m1AScore had the greatest prognostic value. Different infiltration patterns were observed in the high-/low-risk groups for specific immune cells. Our findings provided evidence in favor of our primary hypothesis that m1A regulators were strongly associated with the immune 'traits' of the TME. Of greater significance, the m1A regulator plays a vital role in controlling gene expression, cellular function, and biological processes. Additionally, it exhibits a strong biological association with the development of tumors, as well as therapeutic response. Screening m1A gene signatures for autoimmune-related genes may have more promising tumor immune relevance and provide new strategies for developing treatment plans and possible therapeutic targets for tumor patients.

Our study was subject to several limitations. Initially, certain clinical molecular features, including the status of O6 methylguanine (O6 Meg) - DNA methyltransferase, have been considered reliable predictors of prognosis in glioma patients and are not included in our study [44,45]. Furthermore, because we lack crucial information such as the status of IDH mutation and 1p/19q co-deletion, we are unable to conduct further analysis on the GEO datasets in our study. Moreover, as a result of the variances between microarray and sequencing methods, there may still be some systematic errors. In addition, our findings were only exclusively examined and scrutinized on historical datasets, without analyzing future datasets. And we only performed preliminary verification of the two stable genes (MSR1 and BIRC5) screened in this analysis. Additional clinically relevant *in vivo* and *in vitro* experiments are needed.

In conclusion, we built a robust m1A-RIGS to predict the prognostic risk of patients with primary LGG, and used this to characterize immune cell infiltration based on risk. These findings indicated that m1A-RIGS may be an effective means for evaluating the prognostic risk of patients with LGG, as may be a promising strategy to progress novel managements and treatments approaches for LGG patients. In addition, BIRC5 and MSR1 may be potential therapeutic targets for LGG.

## Data availability statement

The datasets presented in our study can be found in online repositories. The names of the repository/repositories and accession number(s) can be found in the article/Supplementary Material.

## Funding information

## CRediT authorship contribution statement

**Kunjian Lei:** Writing – original draft, Visualization, Methodology, Data curvature, Conceptualization. **Yilei Sheng:** Writing – review & editing, Writing – original draft, Formal analysis, Data cutting, Conceptualization. **Min Luo:** Writing – original draft, Formal analysis, Data calculation. **Junzhe Liu:** Writing – original draft, Formal analysis, Data calculation. **Chuandong Gong:** Writing – original draft, Formal analysis, Data calculation. **Shigang Lv:** Writing – original draft, Formal analysis, Data cure. **Wei Tu:** Writing – original draft, Formal analysis, Data calculation. **Minhua Ye:** Writing – original draft, Formal analysis, Data calculation. **Miaojing Wu:** Writing – original draft, Formal analysis, Data cure. **Bing xiao:** Writing – original draft, Formal analysis, Data calculation. **Hua Fang:** Writing – original draft, Formal analysis, Data calculation. **Haitao Luo:** Writing – original draft, Formal analysis, Data calculation. **Xinjun Liu:** Writing – original draft, Formal analysis, Data cure. **Xiaoyan Long:** Writing – original draft, Formal analysis, Data cure. **Xingen Zhu:** Writing – review & editing, Writing – original draft. **Kai Huang:** Writing – review & editing, Writing – original draft. **Jingying Li:** Writing – review & editing, Writing – original draft.

## Declaration of competing interest

The authors declare that they have no known competing financial interests or personal relationships that could have appeared to influence the work reported in this paper.

## Acknowledgments

## Appendix A. Supplementary data

Supplementary data to this article can be found online at https://doi.org/10.1016/j.heliyon.2024.e27510.

## References

[1] Q.T. Ostrom, et al., The epidemiology of glioma in adults: a "state of the science" review, Neuro Oncol. 16 (2014) 896–913, https://doi.org/10.1093/neuonc/nou087.

[2] N. Cancer Genome Atlas Research, et al., Comprehensive, integrative genomic analysis of diffuse lower-grade gliomas, N. Engl. J. Med. 372 (2015) 2481–2498, https://doi.org/10.1056/NEJMoa1402121.

[3] D.N. Louis, et al., The 2007 WHO classification of tumours of the central nervous system, Acta Neuropathol. 114 (2007) 97–109, https://doi.org/10.1007/s00401-007-0243-4.

[4] B. Wang, et al., Nanoparticles functionalized with Pep-1 as potential glioma targeting delivery system via interleukin 13 receptor alpha2-mediated endocytosis, Biomaterials 35 (2014) 5897–5907, https://doi.org/10.1016/j.biomaterials.2014.03.068.

[5] R. Chen, M. Smith-Cohn, A.L. Cohen, H. Colman, Glioma subclassifications and their clinical significance, Neurotherapeutics 14 (2017) 284–297, https://doi.org/10.1007/s13311-017-0519-x.

[6] C.J. Lewis, T. Pan, A. Kalsotra, RNA modifications and structures cooperate to guide RNA-protein interactions, Nat. Rev. Mol. Cell Biol. 18 (2017) 202–210, https://doi.org/10.1038/nrm.2016.163.

[7] A.T. Ali, Y. Idaghdour, A. Hodgkinson, Analysis of mitochondrial m1A/G RNA modification reveals links to nuclear genetic variants and associated disease processes, Commun. Biol. 3 (2020) 147, https://doi.org/10.1038/s42003-020-0879-3.

[8] M. Safra, et al., The m1A landscape on cytosolic and mitochondrial mRNA at single-base resolution, Nature 551 (2017) 251–255, https://doi.org/10.1038/nature24456.

[9] C. Zhang, G. Jia, Reversible RNA modification N(1)-methyladenosine (m(1)A) in mRNA and tRNA, Dev. Reprod. Biol. 16 (2018) 155–161, https://doi.org/10.1016/j.gpb.2018.03.003.

[10] X. Li, et al., Base-Resolution mapping reveals distinct m(1)A methylome in nuclear- and mitochondrial-encoded transcripts, Mol. Cell 68 (2017), https://doi.org/10.1016/j.molcel.2017.10.019, 993-1005 e1009.

[11] H. Shi, P. Chai, R. Jia, X. Fan, Novel insight into the regulatory roles of diverse RNA modifications: Re-defining the bridge between transcription and translation, Mol. Cancer 19 (2020) 78, https://doi.org/10.1186/s12943-020-01194-6.

[12] W. Guo, et al., Comprehensive analysis of PD-L1 expression, immune infiltrates, and m6A RNA methylation regulators in esophageal squamous cell carcinoma, Front. Immunol. 12 (2021) 669750, https://doi.org/10.3389/fimmu.2021.669750.

[13] Y.Z. Hong Yg, Y. Chen, T. Liu, Y. Zheng, C. Zhou, G.C. Wu, Y. Chen, J. Xia, R. Wen, W. Liu, Y. Zhao, J. Chen, X. Gao, Z. Chen, The RNA m6A reader YTHDF1 is required for acute myeloid leukemia progression, Cancer Res. 83 (2023 Mar 15) 845–860, https://doi.org/10.1158/0008-5472.

[14] M.Z. Jin, W.L. Jin, The updated landscape of tumor microenvironment and drug repurposing, Signal Transduct. Targeted Ther. 5 (2020) 166, https://doi.org/10.1038/s41392-020-00280-x.

[15] D.F. Quail, J.A. Joyce, Microenvironmental regulation of tumor progression and metastasis, Nat. Med. 19 (2013) 1423–1437, https://doi.org/10.1038/nm.3394.

[16] M. Haist, H. Stege, S. Grabbe, M. Bros, The functional crosstalk between myeloid-derived suppressor cells and regulatory T cells within the immunosuppressive tumor microenvironment, Cancers 13 (2021), https://doi.org/10.3390/cancers13020210.

[17] X. Lei, et al., Immune cells within the tumor microenvironment: biological functions and roles in cancer immunotherapy, Cancer Lett. 470 (2020) 126–133, https://doi.org/10.1016/j.canlet.2019.11.009.

[18] D.S. Vinay, et al., Immune evasion in cancer: mechanistic basis and therapeutic strategies, Semin. Cancer Biol. 35 (Suppl) (2015) S185–S198, https://doi.org/10.1016/j.semcancer.2015.03.004.

[19] S. Jhunjhunwala, C. Hammer, L. Delamarre, Antigen presentation in cancer: insights into tumour immunogenicity and immune evasion, Nat. Rev. Cancer 21 (2021) 298–312, https://doi.org/10.1038/s41568-021-00339-z.

[20] H. Chen, et al., Cross-talk of four types of RNA modification writers defines tumor microenvironment and pharmacogenomic landscape in colorectal cancer, Mol. Cancer 20 (2021) 29, https://doi.org/10.1186/s12943-021-01322-w.

[21] D. Han, et al., Anti-tumour immunity controlled through mRNA m(6)A methylation and YTHDF1 in dendritic cells, Nature 566 (2019) 270–274, https://doi.org/10.1038/s41586-019-0916-x.

[22] T. Liu, et al., The m6A reader YTHDF1 promotes ovarian cancer progression via augmenting EIF3C translation, Nucleic Acids Res. 48 (2020) 3816–3831, https://doi.org/10.1093/nar/gkaa048.

[23] Y. Zhou, et al., Decreased m6A modification of CD34/cd276(B7-H3) leads to immune escape in colon cancer, Front. Cell Dev. Biol. 9 (2021) 715674, https://doi.org/10.3389/fcell.2021.715674.

[24] A. Liberzon, et al., Molecular signatures database (MSigDB) 3.0, Bioinformatics 27 (2011) 1739–1740, https://doi.org/10.1093/bioinformatics/btr260.

[25] B. Li, V. Ruotti, R.M. Stewart, J.A. Thomson, C.N. Dewey, RNA-Seq gene expression estimation with read mapping uncertainty, Bioinformatics 26 (2010) 493–500, https://doi.org/10.1093/bioinformatics/btp692.

[26] G.P. Wagner, K. Kin, V.J. Lynch, Measurement of mRNA abundance using RNA-seq data: RPKM measure is inconsistent among samples, Theor. Biosci. 131 (2012) 281–285, https://doi.org/10.1007/s12064-012-0162-3.

[27] X. Zhang, M. Shi, T. Chen, B. Zhang, Characterization of the immune cell infiltration landscape in head and neck squamous cell carcinoma to aid immunotherapy, Mol. Ther. Nucleic Acids 22 (2020) 298–309, https://doi.org/10.1016/j.omtn.2020.08.030.

[28] R. Gaujoux, C. Seoighe, A flexible R package for nonnegative matrix factorization, BMC Bioinf. 11 (2010) 367, https://doi.org/10.1186/1471-2105-11-367.

[29] G. Yu, L.G. Wang, Y. Han, Q.Y. He, clusterProfiler: an R package for comparing biological themes among gene clusters, OMICS 16 (2012) 284–287, https://doi.org/10.1089/omi.2011.0118.

[30] D.A. Barbie, et al., Systematic RNA interference reveals that oncogenic KRAS-driven cancers require TBK1, Nature 462 (2009) 108–112, https://doi.org/10.1038/nature08460.

[31] P. Charoentong, et al., Pan-cancer immunogenomic analyses reveal genotype-immunophenotype relationships and predictors of response to checkpoint blockade, Cell Rep. 18 (2017) 248–262, https://doi.org/10.1016/j.celrep.2016.12.019.

[32] S. Hanzelmann, R. Castelo, J.G.S.V.A. Guinney, Gene set variation analysis for microarray and RNA-seq data, BMC Bioinf. 14 (2013) 7, https://doi.org/10.1186/1471-2105-14-7.

[33] K. Lei, et al., Prognostic and predictive value of immune-related gene pair signature in primary lower-grade glioma patients, Front. Oncol. 11 (2021) 665870, https://doi.org/10.3389/fonc.2021.665870.

[34] H. Gittleman, A.E. Sloan, J.S. Barnholtz-Sloan, An independently validated survival nomogram for lower-grade glioma, Neuro Oncol. 22 (2020) 665–674, https://doi.org/10.1093/neuonc/noz191.

[35] R. Frazzi, BIRC3 and BIRC5: multi-faceted inhibitors in cancer, Cell Biosci. 11 (2021) 8, https://doi.org/10.1186/s13578-020-00521-0.

[36] H.D. Nguyen, et al., A machine learning analysis of a "normal-like" IDH-WT diffuse glioma transcriptomic subgroup associated with prolonged survival reveals novel immune and neurotransmitter-related actionable targets, BMC Med. 18 (2020) 280, https://doi.org/10.1186/s12916-020-01748-x.

[37] Q. Ji, et al., Comprehensive analysis of the prognostic and role in immune cell infiltration of MSR1 expression in lower-grade gliomas, Cancer Med. (2022), https://doi.org/10.1002/cam4.4603.

[38] L. Shi, et al., Expression and significance of m1A transmethylase, hTrm6p/hTrm61p and its related gene hTrm6/hTrm61 in bladder urothelial carcinoma, Am. J. Cancer Res. 5 (2015) 2169–2179.

[39] Y. Zhao, et al., m1A regulated genes modulate PI3K/AKT/mTOR and ErbB pathways in gastrointestinal cancer, Transl Oncol 12 (2019) 1323–1333, https://doi.org/10.1016/j.tranon.2019.06.007.

[40] Z. Chen, et al., Transfer RNA demethylase ALKBH3 promotes cancer progression via induction of tRNA-derived small RNAs, Nucleic Acids Res. 47 (2019) 2533–2545, https://doi.org/10.1093/nar/gky1250.

[41] Y. Gao, et al., Integrated analyses of m(1)A regulator-mediated modification patterns in tumor microenvironment-infiltrating immune cells in colon cancer, OncoImmunology 10 (2021) 1936758, https://doi.org/10.1080/2162402X.2021.1936758.

[42] J. Liu, et al., Comprehensive of N1-methyladenosine modifications patterns and immunological characteristics in ovarian cancer, Front. Immunol. 12 (2021) 746647, https://doi.org/10.3389/fimmu.2021.746647.

[43] F. Macari, et al., TRM6/61 connects PKCalpha with translational control through tRNAi(Met) stabilization: impact on tumorigenesis, Oncogene 35 (2016) 1785–1796, https://doi.org/10.1038/onc.2015.244.

[44] E. Lechapt-Zalcman, et al., O(6) -methylguanine-DNA methyltransferase (MGMT) promoter methylation and low MGMT-encoded protein expression as prognostic markers in glioblastoma patients treated with biodegradable carmustine wafer implants after initial surgery followed by radiotherapy with concomitant and adjuvant temozolomide, Cancer 118 (2012) 4545–4554, https://doi.org/10.1002/cncr.27441.

[45] N. Thon, S. Kreth, F.W. Kreth, Personalized treatment strategies in glioblastoma: MGMT promoter methylation status, OncoTargets Ther. 6 (2013) 1363–1372, https://doi.org/10.2147/OTT.S50208.